



ELSEVIER

Contents lists available at ScienceDirect

Free Radical Biology and Medicine

journal homepage: www.elsevier.com/locate/freeradbiomed

Original Contribution

Antisense oligonucleotide against GSK-3 β in brain of SAMP8 mice improves learning and memory and decreases oxidative stress: Involvement of transcription factor Nrf2 and implications for Alzheimer disease



Susan A. Farr^{a,1}, Jessica L. Ripley^{b,1}, Rukhsana Sultana^b, Zhaoshu Zhang^b, Michael L. Niehoff^a, Thomas L. Platt^c, M. Paul Murphy^c, John E. Morley^{a,d}, Vijaya Kumar^{a,e}, D. Allan Butterfield^{b,*}

^a Research & Development Service, VA Medical Center, St. Louis, MO, USA

^b Department of Chemistry, Center of Membrane Sciences, Sanders Brown Center on Aging, University of Kentucky, Lexington, KY 40506, USA

^c Sanders-Brown Center on Aging, University of Kentucky, Lexington, KY 40536, USA

^d Division of Endocrinology, Saint Louis University School of Medicine, St. Louis, MO, USA

^e Division of Geriatric Medicine, Saint Louis University School of Medicine, St. Louis, MO, USA

ARTICLE INFO

Article history:

Received 24 July 2013

Received in revised form

12 November 2013

Accepted 14 November 2013

Available online 16 December 2013

Keywords:

Alzheimer's disease (AD)

Glycogen synthase kinase-3 β (GSK-3 β)

Nuclear factor-E2-related factor 2 (Nrf2)

Antisense

SAMP8 mice

Oxidative stress

ABSTRACT

Glycogen synthase kinase (GSK)-3 β is a multifunctional protein that has been implicated in the pathological characteristics of Alzheimer's disease (AD), including the heightened levels of neurofibrillary tangles, amyloid-beta (A β), and neurodegeneration. In this study we used 12-month-old SAMP8 mice, an AD model, to examine the effects GSK-3 β may cause regarding the cognitive impairment and oxidative stress associated with AD. To suppress the level of GSK-3 β , SAMP8 mice were treated with an antisense oligonucleotide (c AO) directed at this kinase. We measured a decreased level of GSK-3 β in the cortex of the mice, indicating the success of the antisense treatment. Learning and memory assessments of the SAMP8 mice were tested post-antisense treatment using an aversive T-maze and object recognition test, both of which observably improved. In cortex samples of the SAMP8 mice, decreased levels of protein carbonyl and protein-bound HNE were measured, indicating decreased oxidative stress. Nuclear factor erythroid-2-related factor 2 (Nrf2) is a transcription factor known to increase the level of many antioxidants, including glutathione-S transferase (GST), and is negatively regulated by the activity of GSK-3 β . Our results indicated the increased nuclear localization of Nrf2 and level of GST, suggesting the increased activity of the transcription factor as a result of GSK-3 β suppression, consistent with the decreased oxidative stress observed. Consistent with the improved learning and memory, and consistent with GSK-3 β being a tau kinase, we observed decreased tau phosphorylation in brain of c AO-treated SAMP8 mice compared to that of r AO-treated SAMP8 mice. Lastly, we examined the ability of c AO to cross the blood-brain barrier and determined it to be possible. The results presented in this study demonstrate that reducing GSK-3 with a phosphorothionated antisense against GSK-3 improves learning and memory, reduces oxidative stress, possibly coincident with increased levels of the antioxidant transcriptional activity of Nrf2, and decreases tau phosphorylation. Our study supports the notion of c AO as a possible treatment for AD.

© 2013 Elsevier Inc. All rights reserved.

Abbreviations: A β , amyloid-beta; AD, Alzheimer's disease; BBB, blood-brain barrier; BSA, bovine serum albumin; GSK-3 β , glycogen synthase kinase-3 β ; GST, glutathione S-transferase; ICV, intracerebroventricularly; NFTs, neurofibrillary tangles; Nrf2, nuclear factor-E2-related factor 2; PS-1, presenilin-1

* Corresponding author. Fax: +1 859 323 1464.

E-mail address: dabcns@uky.edu (D.A. Butterfield).

¹ Co-first authors.

Introduction

Alzheimer's disease (AD) is a neurodegenerative disease that, according to the Alzheimer's Association website [1], affects 5.4 million Americans today, costing an estimated \$200 billion in 2012 to care for these individuals. Pathologically, AD is characterized by the accumulation of neurofibrillary tangles (NFTs) and amyloid-beta (A β) plaques, two primary hallmarks of the disease, as well as a heightened oxidative environment in the brain and

subsequent neurodegeneration. Clinically, individuals affected by AD experience a progressive cognitive decline in learning and memory which eventually leads to a highly compromised quality of life. A β -oligomers and NFTs are associated with the cognitive decline characteristic of the disorder [2]. To date there is no treatment which can stop or reverse the dysfunctions produced by the disorder.

Glycogen synthase kinase (GSK)-3 β is a pleiotropic enzyme involved in a variety of cell activities, and has been postulated as a therapeutic target for AD due to its multiple connections to the pathology of the disease [3,4]. Brains from Alzheimer's subjects reportedly have increased GSK-3 β -associated NFTs, tau phosphorylation, and neurodegeneration [5–12]. There are two isoforms of GSK-3, α and β , both of which reportedly elicit an increase in A β [8,13–17]. However, the involvement of GSK-3 in the phosphorylation of presenilin-1 (PS-1) which leads to increased production of A β is unclear [18]. In the brain, GSK-3 β is the predominant kinase that phosphorylates tau, resulting in the hyperphosphorylation and related NFT generation of AD [19–23].

Antioxidant transcription factor nuclear factor-E2-related factor 2 (Nrf2) is among the many substrates negatively regulated by GSK-3 β and is thought to have neuroprotective effects [24–27]. The main role of Nrf2 is to protect the cell against increased oxidative insults and thought to be regulated by cellular localization. In the absence of oxidative stress Nrf2 is bound to the chaperone protein Keap1, which sequesters the transcription factor in the cytosol [28–30]. During increased oxidative insults, Nrf2 disassociates from Keap1 and translocates to the nucleus where it up-regulates the transcription of over a hundred antioxidant genes, mainly phase II enzymes such as glutathione S-transferase (GST), γ -glutamylcysteine ligase, heme oxygenase-1, and glutathione peroxidase [31,32].

The SAMP8 mouse is a model of AD that develops deficits in learning and memory by 8 months of age [33,34]. Correlated with the cognitive impairments, SAMP8 mice exhibit an age-related increase in A β , tau phosphorylation, and oxidative stress [35–38]. The cognitive deficits can be reversed by lowering A β with antisense directed at APP [35,39]. More recently, treatments that reduce GSK have been found to improve learning and memory, and decrease oxidative stress in SAMP8 mice [40].

We have developed an antisense oligonucleotide that targets GSK-3 β to determine if disrupting the activity of GSK-3 β will improve learning and memory in the SAMP8 mouse, a model of AD. We determined that the antisense could improve learning and memory when administered intracerebroventricularly (ICV). At the completion of the learning and memory testing, the cortex was collected and analyzed for GSK levels and oxidative stress. Upon cellular fractionalization, we measured nuclear and cytosolic levels of Nrf2 to examine the possible effects its GSK-3 β -induced inhibition may have on the increased oxidative status associated with this model of AD. Transcriptional activity of Nrf2 was assessed through analyzing the level of GST in the homogenized samples. Finally, we examined the ability of the antisense to cross the blood–brain barrier (BBB).

Materials and methods

Animal subjects

At the start of treatment, the subjects for the experiments were 11-month-old SAMP8 mice from our breeding colony. Sentinels from the facility were tested regularly to ensure that our facility is virus and pathogen free. Food (Richland 5001) and water were available on an *ad libitum* basis and the rooms had a 12 h light–dark

cycle with lights on at 0600 h. Behavioral experiments were conducted between 0730 and 1100 h.

Antisense

GSK antisense oligonucleotide ($_G$ AO) [sequence: 5' (P=S) GGTT-ACCTTGCTGCCATCTT-3'] or random antisense ($_R$ AO) (sequence: GAT-CACGTACACATCGACACCAGTCGCCATGACTGAGCTT) (Midland Certified Reagent Company, Midland, TX) was synthesized. Mice received 3 treatments of the respective antisenses dissolved in saline at 1-week intervals ICV.

Surgery and drug administration

Forty-eight hours prior to training, mice were anesthetized with 4% isoflurane and placed in a stereotaxic instrument, the scalp was deflected, and a hole was drilled through the skull over the injection site. The injection coordinates for the ICV injections were 0.5 mm posterior to the Bregma and 1.0 mm to the right of the sagittal suture. The injection depth was 2.0 mm. As noted, mice were injected 3 times at 1-week intervals. After ICV injection, the scalp was closed and the mice were returned to their cages.

In this study, cortical brain regions were collected from SAMP8 mice treated with GAO ($n = 9$) and $_R$ AO ($n = 7$), the latter serving as the control.

Chemicals and materials

All chemicals were of the highest purity and purchased from Sigma-Aldrich (St. Louis, MO, USA) unless stated otherwise. Nitrocellulose membranes, polyacrylamide gels, XT MES electrophoresis running buffer, and Precision Plus Protein, and all Blue Standards were purchased from Bio-Rad (Hercules, CA).

Behavioral testing

T-maze training and testing procedures

Acquisition was tested 5 days after the third injection in an aversive T-maze. The T-maze is both a learning task based on working-memory and a reference-memory task. The T-maze consisted of a black plastic alley with a start box at one end and two goal boxes at the other. The start box was separated from the alley by a plastic guillotine door that prevented movement down the alley until raised at the onset of training. An electrifiable floor of stainless-steel rods ran throughout the maze to deliver a mild scrambled foot shock.

Mice were not permitted to explore the maze prior to training. A block of training trials began when a mouse was placed into the start box. The guillotine door was raised and a cue buzzer sounded simultaneously; 5 s later foot shock was applied. The arm of the maze entered on the first trial was designated “incorrect” and the mild foot shock was continued until the mouse entered the other goal box, which in all subsequent trials was designated as “correct” for the particular mouse. At the end of each trial, the mouse was returned to its home cage until the next trial.

Mice were trained until they made 1 avoidance. Training used an intertrial interval of 35 s, the buzzer was of the door-bell type sounded at 55 dB, and shock was set at 0.35 mA (Coulbourn Instruments Model E13-08scrambled grid floor shocker). Retention was tested 1 week later by continuing training until mice reached the criterion of 5 avoidances in 6 consecutive trials. The results were reported as the number of trials to criterion for the retention test.

Object-place recognition

Object recognition was tested the 3 days following retention testing. Object-place recognition is a declarative memory task that involves the hippocampus when, as performed here, the retention interval is 24 h after initial exposure to the objects [41]. Mice were habituated to an empty apparatus for 5 min a day for 3 days prior to entry of the objects. During the training session, the mouse was exposed to two similar objects (plastic frogs) which it was allowed to examine for 5 min. The apparatus and the objects were cleaned between each mouse. Twenty-four hours later, the mouse was exposed to one of the original objects and a new novel object in a new location and the percentage of time spent examining the new object was recorded. The novel object was made out of the same material as the original object and of the same size, but a different shape. This eliminated the possibility of smell associated with a particular object being a factor. The underlying concept of the task is based on the tendency of mice to spend more time exploring new, novel objects than familiar objects. Thus, the greater the retention/memory at 24 h, the more time spent with the new object.

Sample preparation for GSK-3 β and oxidative stress measurements

Brain samples were briefly homogenized with a Wheaton tissue homogenizer in an ice-cold lysis buffer (pH 7.4) containing 320 mM sucrose, 1% mM Tris-HCl (pH 8.8), 0.098 mM MgCl₂, 0.076 mM EDTA, and proteinase inhibitors leupeptin (0.5 mg/ml), pepstatin (0.7 μ g/ml), aprotinin (0.5 mg/ml), and PMSF (40 μ g/ml) and a phosphatase inhibitor cocktail. The homogenized samples were then diluted 2X with lysis buffer. After homogenization, a small aliquot of homogenized samples was sonicated for 10 s at 20% power with a Fisher 550 Sonic Dismembrator (Pittsburgh, PA, USA) and frozen. The remaining homogenate was centrifuged at 3000 g for 5 min and the supernatant cytosolic and membranous fractions were transferred out into another set of tubes. Following the addition of 400 μ l of lysis buffer, the remaining pellet nuclear fraction was centrifuged at 3000 g for 5 min and supernatant removed. The pellet was suspended in 20 μ l of lysis buffer and inhibitor. The supernatant cytosolic and membranous fractions were centrifuged at 10,000 g for 10 min, and the resulting supernatant cytosolic fraction was transferred out into another set of tubes leaving the pellet membranous fraction. All sonicated samples and fractions were stored at -70°C until used for further experiments. Protein concentrations were measured through Pierce bicinchoninic acid (BCA) method [42].

Slot blot analysis

Protein carbonyl detection

Protein carbonyls are an index of protein oxidation [37]. For protein carbonyl detection, slot blot analysis of the 2,4-dinitrophenyl hydrazone (DNP) Schiff-base adduct of the carbonyls was employed. Sample aliquots of 5 μ l were incubated at room temperature with 5 μ l of 12% sodium dodecyl sulfate and 10 μ l of 2,4-dinitrophenylhydrazine (from OxyBlot™ Protein oxidation kit, Chemicon-Millipore, Billerica, MA, USA) for 20 min, followed by the addition of 7.5 μ l of neutralization solution containing Tris (2 M) in 30% glycerol to each sample. Following derivatization samples were diluted to 1 μ g/ml using 1X phosphate buffer solution (PBS) containing sodium chloride, and mono and dibasic sodium phosphate. The corresponding sample solutions (250 μ l) were rapidly loaded as duplicates onto a nitrocellulose membrane through water vacuum pressure. The resulting protein-bound nitrocellulose membrane was then blocked with fresh blocking solution containing 750 mg of bovine serum albumin (BSA) in 25 ml of wash blot containing 35.2 g sodium chloride, 1.77 g

monobasic sodium phosphate, 9.61 g dibasic sodium phosphate, and 1.6 ml Tween, diluted to 4 L with deionized water for 90 min. The membrane was then incubated with polyclonal RbxDNP (from OxyBlot™ Protein oxidation kit, Chemicon-Millipore, Billerica, MA, USA, dilution 1:100) in wash blot for 2 h. After three 5-min washes with fresh wash blot, the membrane was then incubated with polyclonal anti-rabbit IgG alkaline phosphatase (Chemicon, Temecula, CA, USA, dilution 1:8000) for 1 h and washed with fresh wash blot in three increments of 5, 10, and 10 min. After washing, the membrane was developed colorimetrically using a 5-bromo-4-chloro-3-indolyl-phosphate/nitroblue tetrazolium reagent solution for alkaline phosphatase secondary antibody. After development, blots were dried and scanned on a CanoScan8800F (Canon) scanner using Adobe Photoshop and analyzed using Scion Image software (Scion Corporation).

Protein-bound HNE detection

Protein-bound HNE is an index of lipid peroxidation [43]. For slot blot analysis of protein-bound HNE detection, sample aliquots of 5 μ l were incubated at room temperature with 5 μ l of 12% sodium dodecyl sulfate and 10 μ l of Laemmli buffer for 20 min, followed by dilution to 1 μ g/ml using 1X phosphate buffer solution (PBS) containing sodium chloride and mono and dibasic sodium phosphate. The corresponding sample solutions (250 μ l) were rapidly loaded as duplicates onto a nitrocellulose membrane through water vacuum pressure. The resulting protein-bound nitrocellulose membrane was then blocked with fresh blocking solution for 90 min. The membrane was then incubated with polyclonal anti-HNE (Alpha Diagnostic, San Antonio, TX, USA, dilution 1:5000) in wash blot for 2 h. After three 5-min washes with fresh wash blot, the membrane was then incubated with polyclonal anti-rabbit IgG alkaline phosphatase (Chemicon, Temecula, CA, USA, dilution 1:8000) for 1 h and washed with fresh wash blot in three increments of 5, 10, and 10 min. After washing, the membrane was developed colorimetrically using a 5-bromo-4-chloro-3-indolyl-phosphate/nitroblue tetrazolium reagent solution for alkaline phosphatase secondary antibody. After development, blots were dried and scanned on a CanoScan8800F (Canon) scanner using Adobe Photoshop and analyzed using Scion Image software (Scion Corporation).

Western blot analysis

The Western blot technique was used to measure protein levels of GSK-3 β , Nrf2, phospho-tau, and GST. For Western blot, 30 or 50 μ g of protein was combined with loading buffer containing 0.5 M Tris (pH 6.8), 40% glycerol, 8% SDS, 20% β -mercaptoethanol, and 0.01% bromophenol blue, denatured in boiling water for 5 min, and then cooled on ice. Sample proteins were resolved on a 4–12% Bis-Tris polyacrylamide gel at room temperature using a Criterion Cell vertical electrophoresis buffer tank filled with 1X XT MES running buffer. During the electrophoretic run, the voltage was initially set at 80 V for \sim 10 min, to ensure proper protein stacking, and then increased to 120 V for \sim 130 min. The voltage of the phospho-tau measurement was 170 V for 80 min. The separated proteins from the gel were then transferred to nitrocellulose membrane using a Trans-Blot Turbo transfer system SD semi-dry transfer cell (Bio-Rad) at 1.0 A/gel for 30 min, while 80 min was applied for phospho-tau transference. The protein transfer from the gel to the membrane was checked using the reversible protein stain, ponceau S.

The subsequent protein-bound membranes were incubated for 90 min in fresh blocking buffer, and then incubated for 3 h in dilutions of primary anti-GSK-3 β (rabbit, Cell Signaling, Danvers, MA, USA, dilution 1:2000), anti-Nrf2 (rabbit, Enzo Life Sciences,

Farmingdale, NY, USA, dilution 1:1000), AT180 (Pierce, Rockford, IL, USA, dilution 1:1000), and anti-GST (rabbit, Epitomics, Burlingame, CA, USA, dilution 1:1000) prepared in fresh wash blot. Subsequent membranes were then washed three times with fresh wash blot and incubated for 1 h in a dark room with the ECL Plex CyDye-conjugated secondary antibodies (GE Healthcare, Pittsburgh, PA, USA), Cy5 (anti-mouse), and Cy3 (anti-rabbit). Membranes were washed again with fresh wash blot three times. Bands were visualized using a fluorescent laser Typhoon FLA9500 (Cy5, $\lambda_{EX}=633$ nm $\lambda_{EM}=67$; Cy3, $\lambda_{EX}=532$ nm $\lambda_{EM}=570$; GE Healthcare, Pittsburgh, PA, USA) scanner and quantified using Scion Image software (Scion Corporation). The membrane incubated with AT180 primary antibody for phospho-tau was subsequently incubated with anti-mouse HRP secondary antibody (Pierce, Rockford, IL, USA, dilution 1:20000) for 1 h. Bands were visualized using SuperSignal West Dura chemiluminescent substrate (Pierce, Rockford, IL, USA) and exposed to X-Ray film. Bands were quantified using ImageJ software. For loading control, the blots were probed with anti- β -actin (dilution 1:2000), anti-GAPDH (Abcam, Cambridge, MA, USA, dilution 1:1000), or anti-histone 2B (EMD Millipore, Billerica, MA, USA, dilution 1:1000) raised in mouse, followed by incubation with anti-mouse secondary antibody (Cy3).

Blood–brain-barrier influx

Labeling of cAO

The anti-GSK was labeled with ^{32}P as previously described [44]. Briefly, cAO anti-GSK was end-labeled by mixing 5 μ g of cAO with 3 μ l of 10X kinase buffer, 1.5 μ l of T4 polynucleotide kinase, and 3 μ l of [γ - ^{32}P]ATP. Following incubation and subsequent kinase heat inactivation, the labeled ^{32}P - cAO (P - cAO) was removed from the reaction mixture by ethanol precipitation followed by centrifugation. The pellet containing the P - cAO went through three cycles of washing with ethanol and centrifugation, and then the pellet was air-dried in a vacuum centrifuge and resuspended in 100 μ l water.

Clearance from serum

Male CD-1 mice 4 months of age were anesthetized with an ip injection of 0.2 ml urethane. The jugular vein and carotid artery were exposed. Each mouse was given a 0.2-ml injection into the jugular vein of saline solution containing 1% bovine serum albumin(S-BSA) and 3×10^5 CPM P - cAO . At time points of 1, 2, 3, 4, 5, 7.5, 10, 15, 20, 30, 60, or 120 min postinjection, carotid arterial blood was collected, the mouse immediately decapitated, and the brain removed and weighed. Arterial blood was centrifuged and 3600 rpm for 15 min and the serum was collected. The level of radioactivity in serum and brain was determined with a scintillation counter. The rate of clearance of P - cAO P -GSK from the serum was determined by expressing the results as the percentage of the injected dose in each milliliter of serum (%Inj/ml) and plotting these values against time (min). The %Inj/ml was determined by the equation:

$$\%Inj/ml = (CPM/ml \text{ serum}) / (\text{mean CPM}/\text{injection})100.$$

Blood to brain passage of P - cAO

Multiple-time regression analysis was used to determine the rate of uptake from blood to brain for P - cAO . The brain/serum ratios (B/S) were calculated for each time point ranging from 1 to 120 min after iv injection of P - cAO for the extended curve ($n=1/\text{time point}$) and 1 to 20 min after iv injection for the short curve ($n=1-2/\text{time point}$). These ratios were plotted against their respective exposure times (Expt). From this graph, the slope of the linear portion of the line represents the unidirectional influx

rate (K_i) and the y -intercept represents the initial volume of distribution (V_i). The B/S was calculated using the formula:

$$B/S = (\text{Brain CPM}/\text{g of brain}) / (\text{serum CPM}/\mu\text{l of serum}).$$

Expt was calculated using the formula:

Expt = $\int_0^t Cp(t)dt / Cpt$, where t is time, Cp is the level of radioactivity in the serum and Cpt is the level of radioactivity in the serum at time t ; units = min.

The percentage of the injected dose taken up by each gram of brain tissue (%Inj/g) was calculated as:

$$\%Inj/g = (B/S - V_i)(\%Inj/ml) / 1000.$$

Capillary depletion of P - cAO

This study was performed to determine the distribution of the P - cAO between the brain tissue and the brain capillaries. The procedure has been previously described [45]. Mice ($n=7$) were anesthetized with 40% urethane and then received and iv injection of 1×10^6 CPM of P - cAO in 0.2 ml S-BSA into the jugular vein. Ten minutes postinjection the abdomen was opened and blood collected from the abdominal aorta. The thorax was then opened through a midline sternal incision, the descending aorta clamped, both jugular veins were severed and washout of the vascular space was performed by injecting 20 ml of saline into the left ventricle of the heart over a 1-min period. This procedure washed out the vascular space of the brain, by removing any substances that were intravascular or loosely adhered to the capillary lumen of the brain microvasculature. The brain was then removed and placed in a glass homogenizer containing 0.8 ml of physiologic buffer. After 10 strokes with the pestle, 1.6 ml of the physiologic buffer containing 26% dextran was added to the homogenate. The homogenate was homogenized a second time (3 strokes). The homogenate was centrifuged at 4000 g for 30 min at 4 °C in a swinging bucket rotor. The supernatant (brain parenchyma) was separated from the pellet (brain microvasculature) and the levels of radioactivity were determined. The results were expressed as the volume of distribution in microliters per gram in tissue (parenchyma or capillary)/serum ratios with the formula:

$$\mu\text{l}/\text{g} = (\text{CPM}/\text{gram of tissue}) / (\text{CPM}/\text{ml of serum}).$$

Statistical analysis

Results from the T-maze were analyzed by a t test. Results from the GSK and oxidative stress measurements were compared by the Mann-Whitney test using Prism 5.0 statistical package software to assess statistical significance in comparing protein carbonyl, protein-bound HNE, GSK-3 β , Nrf2, and GST levels in protein samples between control and experimental data sets. Significant differences were set at $P < 0.05$.

Results

Effects of cAO on learning and memory

Seventy-two hours after cAO treatment mice were tested in T-maze foot-shock avoidance acquisition. One week later, the mice were tested for retention. The t test for trial to first avoidance during acquisition in the T-maze showed a significant effect $t(15)=2.092$, $P < 0.05$. The mice that received cAO took significantly fewer trials to reach their first avoidance (8.75 ± 1.22) than the mice that received random antisense (11.67 ± 0.745) (Fig. 1A). The t test for trials to criterion on the retention test showed a significant effect $t(14)=2.945$, $P < 0.01$ (Fig. 1B). The mice that received cAO (6.714 ± 0.42) took significantly fewer trials to reach criterion than the mice that received rAO (12.89 ± 1.806).

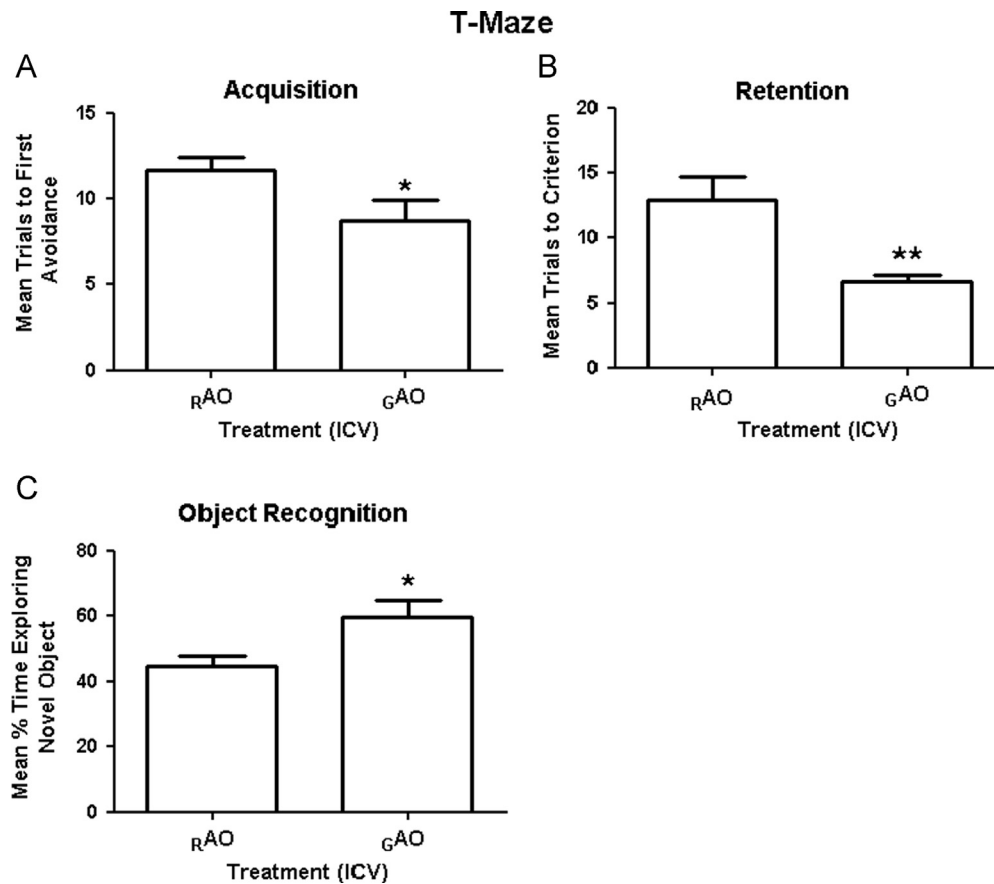


Fig. 1. Antisense oligonucleotide treatment led to improved cognition in 12-month-old SAMP8 mice compared to SAMP8 mice treated with random antisense oligonucleotide. Specifically: The 12-month-old SAMP8 mice which received GAO ($N=9$) took significantly fewer number of trials to make their first avoidance during acquisition (A) and significantly fewer number of trials to make 5 avoidances in 6 consecutive trials on the 1-week retention test (B) in T-maze foot-shock avoidance compared to the 12-month-old SAMP8 mice which received RAO. In the novel object recognition task with a 24-h retention delay the 12-month-old SAMP8 mice that received GAO spent significantly greater percentage of the total exploration time exploring the novel object during the retention test compared to the 12-month-old SAMP8 mice that received RAO ($N=8$) (C), * $P < 0.05$; ** $P < 0.01$.

The t test for time exploring the novel object during the 24-h retention test was significant $t(15)=2.373$, $P < 0.03$. The mice that received c AO (59.33 ± 5.16) spent a significantly greater amount of time exploring the novel object than the mice that received random antisense (44.75 ± 2.93) (Fig. 1C).

Measurement of nuclear and cytosolic GSK-3 β

Immunochemical methods were used to determine if the antisense treatment successfully decreased the level of GSK-3 β in SAMP8 mice compared to the control. GSK-3 β was successfully down regulated in the nuclear and cytosolic fractions by the antisense treatment (Fig. 2A and B). Immunoblot analysis of the GSK-3 β levels in aliquots of nuclear (30 μ l) and cytosolic (50 μ l) fractions indicates a significant decrease of 36.9% ($P < 0.04$) and 16.9% ($P < 0.05$), respectively, from SAMP8 c AO mice compared to the control.

Analysis of protein carbonyls

Sensitive immunochemical methods were used to determine if suppression of GSK-3 β in SAMP8 mice had any effect on protein carbonyl levels. The results indicate a decrease in brain protein oxidation as a result of the suppressed GSK-3 β level in SAMP8 mice. Immunoblot analysis of homogenized brain samples indicates a significant 26.3% decrease ($P < 0.02$) in the protein carbonyl level from SAMP8 c AO mice compared to the control (Fig. 3A).

Analysis of protein-bound HNE

Our results indicate a decreased lipid peroxidation as a result of the suppressed GSK-3 β level in SAMP8 mice brain. Immunoblot analysis of homogenized samples shows a significant 20.3% decrease ($P < 0.0008$) in SAMP8 c AO mice compared to the control (Fig. 3B).

Measurement of nuclear and cytosolic Nrf2

To determine if the suppression of GSK-3 β in SAMP8 mice had an effect on the nuclear translocation of Nrf2, nuclear and cytosolic levels of this redox-sensitive transcription factor were measured. Nrf2 band intensities of the nuclear and cytosolic fractions were normalized to histone-2B and β -actin, respectively, each serving as a loading control. Our results suggest a possible increase in the translocation of Nrf2 from the cytosol to the nucleus as a result of the suppressed GSK-3 β level in SAMP8 mice. Immunoblot analysis of the Nrf2 levels in aliquots of nuclear and cytosolic fractions indicates a significant 69.4% increase ($P < 0.04$) and 29.5% increase ($P < 0.02$), respectively, from SAMP8 c AO mice compared to the control (Fig. 4A and B).

Measurement of GST

GST is one of several antioxidant enzymes up-regulated by Nrf2 transcriptional activity. As a means of determining Nrf2 transcriptional activity, the level of GST was measured. GST band intensities of the homogenized samples were normalized to β -actin, a loading

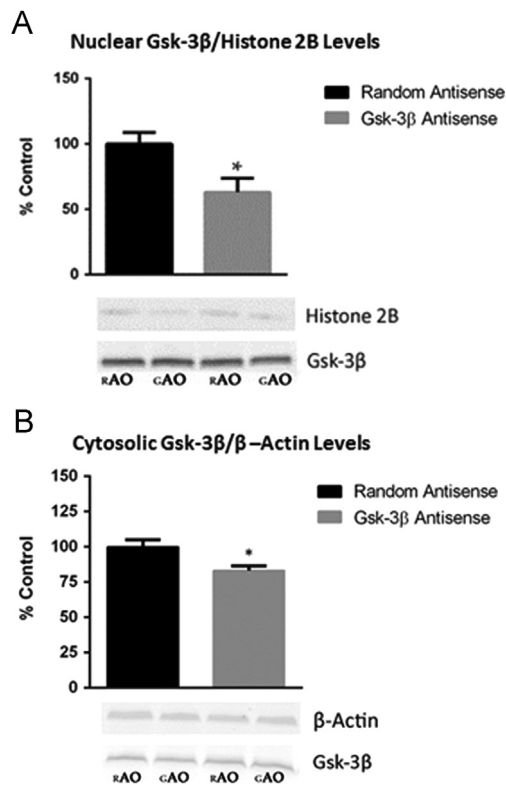


Fig. 2. (A) Nuclear GSK-3 β level in c AO compared to r AO SAMP8 mice. Level of GSK-3 β decreased in the nuclear fraction of SAMP8 mice treated with c AO compared to that of SAMP8 mice treated with r AO. Data are represented as % control, and shown as mean \pm SEM with $*P < 0.04$. Total number of animals used in each group are c AO=5 and r AO=5. (B) Cytosolic GSK-3 β level in c AO compared to r AO SAMP8 mice. Level of GSK-3 β decreased in the cytosolic fraction of SAMP8 mice treated with c AO compared to that of SAMP8 mice treated with r AO. Data are represented as % control, and shown as mean \pm SEM with $*P < 0.05$. Total number of animals used in each group are c AO=8 and r AO=7.

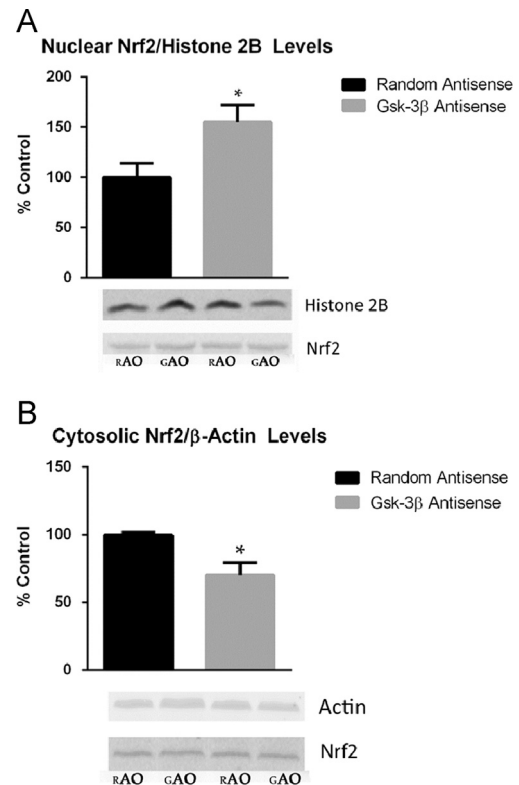


Fig. 4. (A) Nuclear Nrf2 level in c AO compared to r AO SAMP8 mice. The level of Nrf2 increased in the nuclear fraction of SAMP8 mice treated with c AO compared to that of SAMP8 mice treated with r AO. Data are represented as % control, and shown as mean \pm SEM with $*P < 0.04$. Total number of animals used in each group are c AO=5 and r AO=5. (B) Cytosolic Nrf2 level in c AO compared to r AO SAMP8 mice. Reduced expression of Nrf2 in the cytosolic fraction of SAMP8 mice treated with c AO compared to that of SAMP8 mice treated with r AO. Data are represented as % control, and shown as mean \pm SEM with $*P < 0.02$. Total number of animals used in each group are c AO=9 and r AO=5.

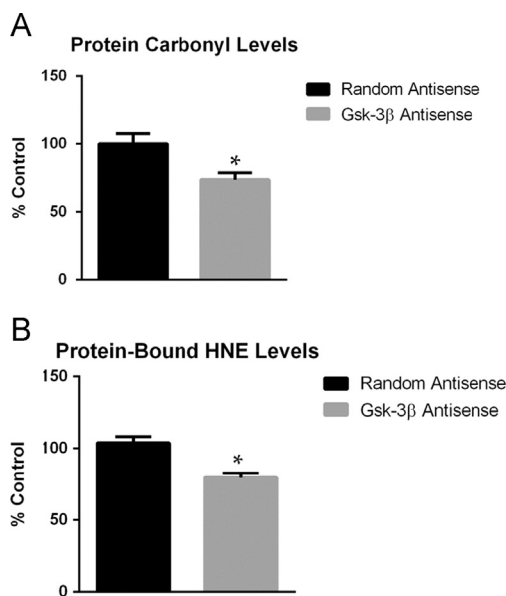


Fig. 3. (A) Protein carbonyl level in c AO compared to r AO SAMP8 mice. Protein carbonyl level decreased in SAMP8 mice treated with AO directed at GSK-3 β ($N=9$) compared to that of SAMP8 mice treated with random AO ($N=7$). Data are represented as % control, and shown as mean \pm SEM with $*P < 0.02$. (B) Protein-bound HNE level in c AO compared to r AO SAMP8 mice. Protein-bound HNE level decreased in SAMP8 mice treated with AO directed at GSK-3 β ($N=9$) compared to that of SAMP8 mice treated with random AO ($N=6$). Data are represented as % control, and shown as mean \pm SEM with $*P < 0.0008$.

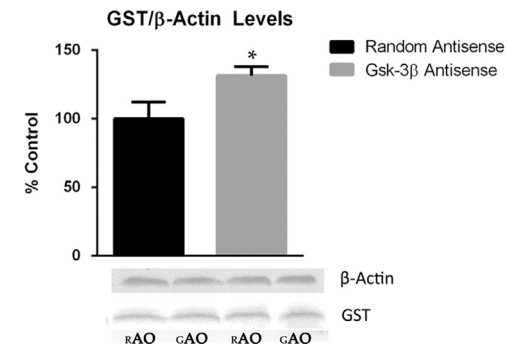


Fig. 5. GST level in c AO compared to r AO SAMP8 mice. The level of GST increased in the homogenized samples of SAMP8 mice treated with c AO compared to that of SAMP8 mice treated with r AO. Data are represented as % control, and shown as mean \pm SEM with $*P < 0.03$. Total number of animals used in each group are c AO=7 and r AO=6.

control. Our results suggest a possible increase in Nrf2 transcriptional activity as a result of the suppressed GSK-3 β level in SAMP8 mice. Immunoblot analysis of the GST level in 30 μ l aliquots of protein sample shows a significant 31.5% increase ($P < 0.03$), from SAMP8 c AO mice compared to the control (Fig. 5).

Measurement of phospho-tau

Given that: (1) GSK-3 β is a kinase for tau; (2) tau hyperphosphorylation is highly detrimental to neurons; and (3) c AO treatment led to improved learning and memory in SAMP8 mice

(Fig. 1), we tested the hypothesis that cAO treatment would result in lower levels of phospho-tau in brain of SAMP8 mice compared to brain from rAO -treated SAMP8 mice. Fig. 6 shows that this hypothesis was confirmed ($P < 0.01$).

cAO influx across the blood–brain barrier

The %Inj/ml demonstrated that there was an early decline of P-cAO from serum. Serum levels reached a steady state by 30 min after iv injection. The early distribution phase of clearance from serum was linear out to 20 min, with a significant correlation between $\log[\% \text{Inj/ml}]$ and time. The half-time disappearance rate from serum was -7.47 min ($r=0.9205$, $P < 0.0001$). The linear relation between the brain/serum ratios (B/S) and the exposure time (Expt) during the first 20 min demonstrated P-cAO influx into the brain. The unidirectional rate of influx (K_i) from blood to brain was $0.2108 \pm 0.0523 \mu\text{l/g-min}$ ($r=0.7722$, $P=0.0020$). The volume of distribution at time zero (V_i) was $6.78 \pm 0.816 \mu\text{l/g}$. When plotted against time, the percentage of the iv injected dose of P-cAO taken up by the brain was $0.033\% \text{Inj/g}$ at 20 min postinjection. Capillary depletion studies produced a mean brain parenchyma/serum ratio of $6.956 \pm 0.995 \mu\text{l/g}$ and a mean capillary/serum ratio of $1.183 \pm 0.163 \mu\text{l/g}$. The parenchyma/serum ratio was almost 6 times greater than the capillary/serum ratio, indicating that the P-cAO completely crossed the BBB to enter the brain parenchymal space (Fig. 7).

Discussion

The regulatory kinase GSK-3 β has been implicated in AD through its various contributions including hyperphosphorylated tau formation and neurodegeneration [6,9,22,23,46]. High levels of GSK-3 β have been reported in AD brain, further supporting a connection between the kinase and the pathogenesis of the neurodegenerative disease that remains to be elucidated [47,48]. In this current study, we examined the possible effects GSK-3 β may have on cognitive deficits and brain oxidative stress observed in a mouse model of AD through the antisense-mediated suppression of the kinase in SAMP8 mice.

The SAMP8 mice used in this study were treated with antisense oligonucleotide directed at GSK-3 β and random antisense oligonucleotide, the latter serving as the control. The GSK-3 β antisense

had a sequence that corresponds to 94–113 nucleotides downstream from the initiation codon of GSK-mRNA. This is an internal sequence with high probability of being located away from any loop formation in the mRNA. As an internal site, it should not block 100% of GSK mRNA. This is important as GSK-3 is essential for intracellular signaling pathways such as cell proliferation, cellular migration, glucose regulation, inflammatory responses, and apoptosis [49]. Analysis of cortical tissue showed a suppression of GSK-3 β , indicating the success of the administered antisense treatment directed at the kinase.

ICV administration of cAO improved learning and memory in T-maze foot-shock avoidance and object recognition in the SAMP8 mouse model of AD, consonant with the notion that this kinase is implicated in the cognitive deficits associated with the disorder. This improved learning and memory was associated with decreased markers of protein oxidation and lipid peroxidation (protein carbonyls and protein-bound HNE, respectively) in brain and was associated with decreased phosphorylation of tau. We measured the levels of protein carbonyl and protein-bound HNE, parameters of protein oxidation and lipid peroxidation, respectively. Both protein carbonyl and protein-bound HNE significantly decreased in brain of cAO -treated SAMP8 mice compared to the control, consistent with the notion that this kinase plays a role in the elevated oxidative status characteristic of AD brain. The observed reduction in oxidative stress may be a consequence of the increased antioxidant transcriptional activity of Nrf2, resulting from its decreased inhibition by GSK-3 β .

The neuroprotective transcription factor Nrf2 is one of the many proteins negatively regulated by the activity of GSK-3 β and this transcription factor plays an important role in the cellular defense against oxidative stress through inducing the expression of antioxidant phase II genes, including, among others, heme oxygenase-1, glutamate-cysteine ligase, and glutathione S-transferase [24,50,51]. To determine if the suppression of GSK-3 β in SAMP8 led to the nuclear relocalization of Nrf2, we measured the nuclear and cytosolic levels of this transcription factor. Significantly increased nuclear and decreased cytosolic Nrf2 levels measured support the increased nuclear localization of the transcription factor. As a means of determining increased transcriptional activity, we measured the level of GST, which is an antioxidant enzyme up-regulated by Nrf2, responsible for the conjugation of HNE to glutathione for export from the brain. The level of GST significantly increased in SAMP8 cAO mice compared to the control, in agreement with the observed decrease in protein-bound HNE, suggesting the increased transcriptional activity of Nrf2. These results support the idea that the activity of GSK-3 β , and its associated inhibition of Nrf2-mediated antioxidant transcription, plays major roles in the loss of tolerance to an oxidative environment observed in AD. As noted, GAO had a neuroprotective effect of reducing phosphorylation of tau compared to treatment with RAO (Fig. 6). Elevated tau phosphorylation is a cardinal hallmark of AD pathology and neurodegeneration. If the activity of GSK-3 β does play a prominent role in the pathogenesis of AD, then inhibitors of the kinase may be an effective therapeutic treatment of the disorder.

Given the critical cellular functions of GSK-3 β , antisense treatment may be an effective way to control the overactivity of the kinase without completely blocking its functions. Currently, there is increasing interest in the use of antisenses for the treatment of diseases. Working through the Watson-Crick mechanism, antisenses bind to and induce the cleavage of homologous stretches of mRNA sequences resulting in the targeted destruction of mRNA [52]. Antisenses are currently in various stages of testing for such conditions as cancer, hypercholesterolemia, Ebola virus infection, type 2 diabetes, HIV infection, and ocular disease, and may be a feasible treatment for AD as well [52,53].

Although the behavioral and oxidative stress studies presented here followed ICV treatment with cAO or rAO , we investigated the

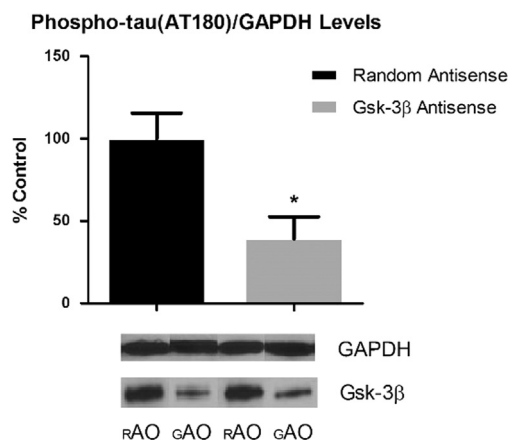


Fig. 6. Phospho-tau (AT180) level in brain of GAO-treated SAMP8 mice compared to RAO-treated SAMP8 mice. The level of phospho-tau (AT180) decreased in the homogenized samples of SAMP8 mice treated with GAO compared to that of SAMP8 mice treated with RAO. Data are represented as % control, and shown as mean \pm SEM with * $P < 0.01$. Total number of animals used in each group are GAO=9 and RAO=7. Shown are two representative Western blots of samples from each group and of GAPDH (loading control).

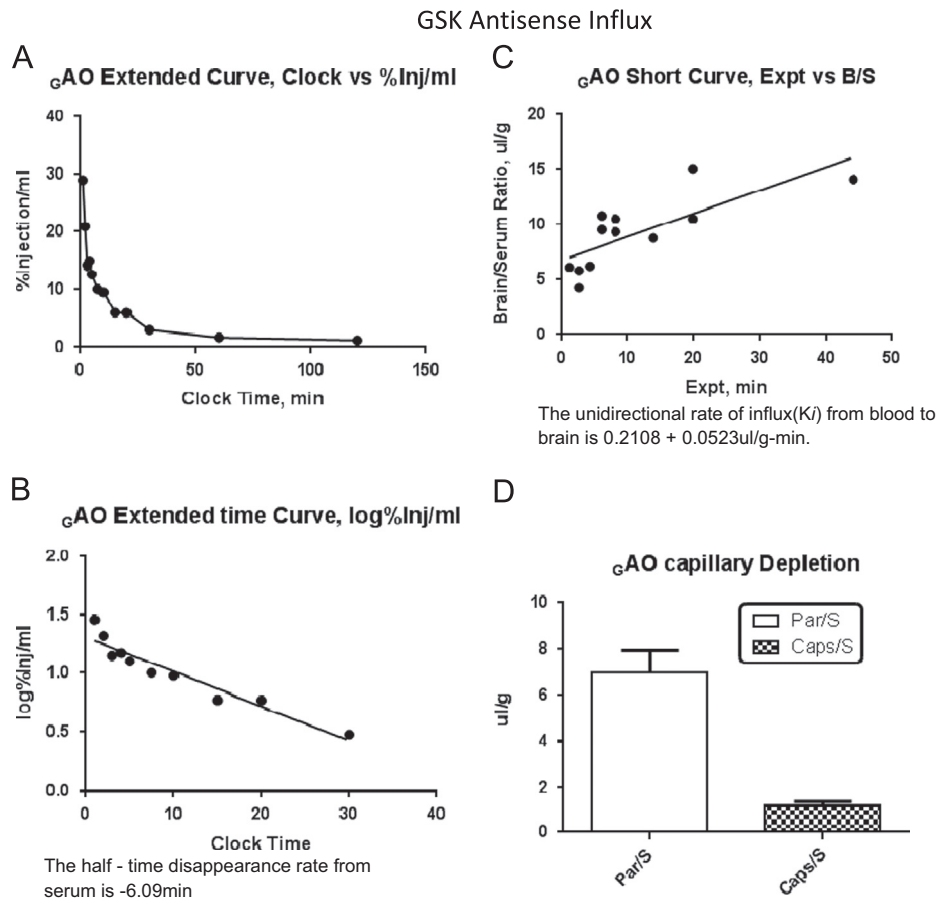


Fig. 7. Kinetics of blood-to-brain transport of ${}^{32}\text{P}$ - c AO after iv administration. (A) Clearance of ${}^{32}\text{P}$ - c AO from blood. (B) The initial distribution phase was linear out to 20 min. (C) Slope of the line with multiple-time regression analysis demonstrated unidirectional influx of ${}^{32}\text{P}$ - c AO with a K_i of $0.2108 \pm 0.0523 \mu\text{l/g}\cdot\text{min}$ and a V_i of $6.78 \pm 0.0816 \mu\text{l/g}$. (D) Capillary depletion demonstrated that ${}^{32}\text{P}$ - c AO crossed the blood–brain barrier to enter the brain parenchyma.

possibility of peripherally administered c AO crossing the BBB, a prerequisite to development of an effective therapy. By examining influx of c AO at the blood–brain barrier, we were able to show that peripherally injected GSK antisense crosses the blood–brain barrier and enters the CNS. These findings with c AO are similar to the findings of an antisense we previously developed directed at the C-terminal portion of the APP peptide (OL-1). We found that administration of OL-1 improved learning and memory, decreased oxidative stress, and crossed the BBB [54–57]. Based on our previous results with APP antisense and our results here with GSK antisense, AD is an additional condition for which antisense likely would be an effective treatment. The current findings in this study suggest that peripheral administration of c AO is feasible and may improve learning and memory and reverse oxidative stress in AD brain.

In conclusion, this paper provides evidence that the inhibition of GSK-3 β with antisense improves cognition and indices of oxidative stress in a mouse model of Alzheimer's disease. In addition, the reduction in Nrf2 provides an additional potential mechanism through which GSK-3 β overactivity contributes to the oxidative damage associated with AD. The ability of c AO to cross the BBB suggests that peripheral administration is possible and that c AO should be investigated further as a potential treatment for AD.

Acknowledgments

This work was supported by a NIH grant to D.A.B. [AG-05119] and grants to S.A.F. [VA Merit Review] and Edunn Biotechnology, St. Louis, MO.

References

- [1] Association, A. S. 2013 Alzheimer's disease facts and figures. *Alzheimer's Dement* **9**:208–245; 2013.
- [2] Clinton, L. K.; Blurton-Jones, M.; Myczek, K.; Trojanowski, J. Q.; LaFerla, F. M. Synergistic Interactions between Abeta, tau, and alpha-synuclein: acceleration of neuropathology and cognitive decline. *J. Neurosci.* **30**:7281–7289; 2010.
- [3] Mondragon-Rodriguez, S.; Perry, G.; Zhu, X.; Moreira, P. I.; Williams, S. Glycogen synthase kinase 3: a point of integration in Alzheimer's disease and a therapeutic target. *Int. J. Alzheimer's Dis.* **2012**:1–4; 2012.
- [4] Woodgett, J. R. Judging a protein by more than its name: GSK-3. *Sci STKE* **2001**:re12; 2001.
- [5] Cho, J. H.; Johnson, G. V. Primed phosphorylation of tau at Thr231 by glycogen synthase kinase 3beta (GSK3beta) plays a critical role in regulating tau's ability to bind and stabilize microtubules. *J. Neurochem.* **88**:349–358; 2004.
- [6] Engel, T.; Goni-Oliver, P.; Lucas, J. J.; Avila, J.; Hernandez, F. Chronic lithium administration to FTDP-17 tau and GSK-3beta overexpressing mice prevents tau hyperphosphorylation and neurofibrillary tangle formation, but pre-formed neurofibrillary tangles do not revert. *J. Neurochem.* **99**:1445–1455; 2006.
- [7] Hooper, C.; Killick, R.; Lovestone, S. The GSK3 hypothesis of Alzheimer's disease. *J. Neurochem.* **104**:1433–1439; 2008.
- [8] Hurtado, D. E.; Molina-Porcel, L.; Carroll, J. C.; Macdonald, C.; Aboagye, A. K.; Trojanowski, J. Q.; Lee, V. M. Selectively silencing GSK-3 isoforms reduces plaques and tangles in mouse models of Alzheimer's disease. *J. Neurosci.* **32**:7392–7402; 2012.
- [9] Lucas, J. J.; Hernandez, F.; Gomez-Ramos, P.; Moran, M. A.; Hen, R.; Avila, J. Decreased nuclear beta-catenin, tau hyperphosphorylation and neurodegeneration in GSK-3beta conditional transgenic mice. *EMBO J.* **20**:27–39; 2001.
- [10] Pei, J. J.; Braak, E.; Braak, H.; Grundke-Iqbal, I.; Iqbal, K.; Winblad, B.; Cowburn, R. F. Distribution of active glycogen synthase kinase 3beta (GSK-3beta) in brains staged for Alzheimer disease neurofibrillary changes. *J. Neuropathol. Exp. Neurol.* **58**:1010–1019; 1999.
- [11] Sereno, L.; Coma, M.; Rodriguez, M.; Sanchez-Ferrer, P.; Sanchez, M. B.; Gich, I.; Agullo, J. M.; Perez, M.; Avila, J.; Guardia-Laguarta, C.; Clarimon, J.; Lleo, A.; Gomez-Isla, T. A novel GSK-3beta inhibitor reduces Alzheimer's pathology and rescues neuronal loss in vivo. *Neurobiol. Dis.* **35**:359–367; 2009.

- [12] Alvarez, G.; Munoz-Montano, J. R.; Satrustegui, J.; Avila, J.; Bogonez, E.; Diaz-Nido, J. Lithium protects cultured neurons against beta-amyloid-induced neurodegeneration. *FEBS Lett.* **453**:260–264; 1999.
- [13] Woodgett, J. R. Molecular cloning and expression of glycogen synthase kinase-3/factor A. *EMBO J.* **9**:2431–2438; 1990.
- [14] Ly, P. T.; Wu, Y.; Zou, H.; Wang, R.; Zhou, W.; Kinoshita, A.; Zhang, M.; Yang, Y.; Cai, F.; Woodgett, J.; Song, W. Inhibition of GSK3 β -mediated BACE1 expression reduces Alzheimer-associated phenotypes. *J. Clin. Invest.* **123**:224–235; 2013.
- [15] Diaz-Hernandez, J. I.; Gomez-Villafuertes, R.; Leon-Otegui, M.; Hontecillas-Prieto, L.; Del Puerto, A.; Trejo, J. L.; Lucas, J. J.; Garrido, J. J.; Gualix, J.; Miras-Portugal, M. T.; Diaz-Hernandez, M. In vivo P2X7 inhibition reduces amyloid plaques in Alzheimer's disease through GSK3 β and secretases. *Neurobiol. Aging* **33**:1816–1828; 2012.
- [16] Ryder, J.; Su, Y.; Liu, F.; Li, B.; Zhou, Y.; Ni, B. Divergent roles of GSK3 and CDK5 in APP processing. *Biochem. Biophys. Res. Commun.* **312**:922–929; 2003.
- [17] Phiel, C. J.; Wilson, C. A.; Lee, V. M.; Klein, P. S. GSK-3 α regulates production of Alzheimer's disease amyloid- β peptides. *Nature* **423**:435–439; 2003.
- [18] Phiel, C. J.; Wilson, C. A.; Lee, V. M.; Klein, P. S. GSK-3 α regulates production of Alzheimer's disease amyloid- β peptides. *Nature* **423**:435; 2003.
- [19] Takashima, A. GSK-3 is essential in the pathogenesis of Alzheimer's disease. *J. Alzheimers Dis.* **9**:309–317; 2006.
- [20] Morris, M.; Maeda, S.; Vossel, K.; Mucke, L. The many faces of tau. *Neuron* **70**:410–426; 2011.
- [21] Hanger, D. P.; Hughes, K.; Woodgett, J. R.; Brion, J. P.; Anderton, B. H. Glycogen synthase kinase-3 induces Alzheimer's disease-like phosphorylation of tau: generation of paired helical filament epitopes and neuronal localisation of the kinase. *Neurosci. Lett.* **147**:58–62; 1992.
- [22] Lovestone, S.; Reynolds, C. H.; Latimer, D.; Davis, D. R.; Anderton, B. H.; Gallo, J. M.; Hanger, D.; Mulot, S.; Marquardt, B.; Stabel, S., et al. Alzheimer's disease-like phosphorylation of the microtubule-associated protein tau by glycogen synthase kinase-3 in transfected mammalian cells. *Curr. Biol.* **4**:1077–1086; 1994.
- [23] Hong, M.; Chen, D. C.; Klein, P. S.; Lee, V. M. Lithium reduces tau phosphorylation by inhibition of glycogen synthase kinase-3. *J. Biol. Chem.* **272**:25326–25332; 1997.
- [24] Shih, A. Y.; Johnson, D. A.; Wong, G.; Kraft, A. D.; Jiang, L.; Erb, H.; Johnson, J. A.; Murphy, T. H. Coordinate regulation of glutathione biosynthesis and release by Nrf2-expressing glia potently protects neurons from oxidative stress. *J. Neurosci.* **23**:3394–3406; 2003.
- [25] Kraft, A. D.; Johnson, D. A.; Johnson, J. A. Nuclear factor E2-related factor 2-dependent antioxidant response element activation by tert-butylhydroquinone and sulforaphane occurring preferentially in astrocytes conditions neurons against oxidative insult. *J. Neurosci.* **24**:1101–1112; 2004.
- [26] Calabrese, V.; Ravagna, A.; Colombrita, C.; Scapagnini, G.; Guagliano, E.; Calvani, M.; Butterfield, D. A.; Giuffrida Stella, A. M. Acetylcarnitine induces heme oxygenase in rat astrocytes and protects against oxidative stress: involvement of the transcription factor Nrf2. *J. Neurosci. Res.* **79**:509–521; 2005.
- [27] Williamson, T. P.; Johnson, D. A.; Johnson, J. A. Activation of the Nrf2-ARE pathway by siRNA knockdown of Keap1 reduces oxidative stress and provides partial protection from MPTP-mediated neurotoxicity. *Neurotoxicology* **33**:272–279; 2012.
- [28] Lo, S. C.; Li, X.; Henzl, M. T.; Beamer, L. J.; Hannink, M. Structure of the Keap1: Nrf2 interface provides mechanistic insight into Nrf2 signaling. *EMBO J.* **25**:3605–3617; 2006.
- [29] Itoh, K.; Wakabayashi, N.; Katoh, Y.; Ishii, T.; Igarashi, K.; Engel, J. D.; Yamamoto, M. Keap1 represses nuclear activation of antioxidant responsive elements by Nrf2 through binding to the amino-terminal Neh2 domain. *Genes Dev.* **13**:76–86; 1999.
- [30] Itoh, K.; Ishii, T.; Wakabayashi, N.; Yamamoto, M. Regulatory mechanisms of cellular response to oxidative stress. *Free Radic. Res.* **31**:319–324; 1999.
- [31] Dinkova-Kostova, A. T.; Holtzclaw, W. D.; Cole, R. N.; Itoh, K.; Wakabayashi, N.; Katoh, Y.; Yamamoto, M.; Talalay, P. Direct evidence that sulfhydryl groups of Keap1 are the sensors regulating induction of phase 2 enzymes that protect against carcinogens and oxidants. *Proc. Natl. Acad. Sci. USA* **99**:11908–11913; 2002.
- [32] Zhang, D. D.; Hannink, M. Distinct cysteine residues in Keap1 are required for Keap1-dependent ubiquitination of Nrf2 and for stabilization of Nrf2 by chemopreventive agents and oxidative stress. *Mol. Cell. Biol.* **23**:8137–8151; 2003.
- [33] Yagi, H.; Katoh, S.; Akiyoshi, I.; Takeda, T. Afe-related deterioration of ability of acquisition in memory and learning in senescence accelerated mouse: SAM-P/8 as an animal model of disturbances in recent memory. *Neurosci. Biobehav. Rev.* **47**:86–93; 1988.
- [34] Flood, J. F.; Morley, J. E. Learning and memory in the SAMP8 mouse. *Neurosci. Biobehav. Rev.* **22**:1–20; 1998.
- [35] Morley, J. E.; Kumar, V. B.; Bernardo, A. I.; Farr, S. A.; Uezu, K.; Tumosa, N.; Flood, J. F. Beta-amyloid precursor polypeptide in SAMP8 mice affects learning and memory. *Peptides* **21**:1761–1767; 2000.
- [36] Pallas, M.; Camins, A.; Smith, M. A.; Perry, G.; Lee, H. G.; Casadesus, G. From aging to Alzheimer's disease: unveiling "the switch" with the senescence-accelerated mouse model (SAMP8). *J. Alzheimers Dis.* **15**:615–624; 2008.
- [37] Butterfield, D. A.; Stadtman, E. R. Protein oxidation processes in aging brain. *Adv. Cell Aging Gerontol.* **161**–191; 1997.
- [38] Poon, H. F.; Castegna, A.; Farr, S. A.; Thongboonkerd, V.; Lynn, B. C.; Banks, W. A.; Morley, J. E.; Klein, J. B.; Butterfield, D. A. Quantitative proteomics analysis of specific protein expression and oxidative modification in aged senescence-accelerated-prone 8 mice brain. *Neuroscience* **126**:915–926; 2004.
- [39] Erickson, M. A.; Niehoff, M. L.; Farr, S. A.; Morley, J. E.; Dillman, L. A.; Lynch, K. M.; Banks, W. A. Peripheral administration of antisense oligonucleotides targeting the amyloid- β protein precursor reverses ABPP and LRP-1 overexpression in the aged SAMP8 mouse brain. *J. Alzheimers Dis.* **28**:951–960; 2012.
- [40] Tajas, M.; Yeste-Velasco, M.; Zhu, X.; Chou, S. P.; Smith, M. A.; Pallas, M.; Camins, A.; Casadesus, G. Activation of Akt by lithium: pro-survival pathways in aging. *Mech. Ageing Dev.* **130**:253–261; 2009.
- [41] Hammond, R. S.; Tull, L. E.; Stackman, R. W. On the delay-dependent involvement of the hippocampus in object recognition memory. *Neurobiol. Learn. Mem.* **82**:26–34; 2004.
- [42] Smith, P. K.; Krohn, R. I.; Hermanson, G. T.; Mallia, A. K.; Gartner, F. H.; Provenzano, M. D.; Fujimoto, E. K.; Goeke, N. M.; Olson, B. J.; Klenk, D. C. Measurement of protein using bicinchoninic acid. *Anal. Biochem.* **150**:76–85; 1985.
- [43] Sultana, R.; Perluigi, M.; Butterfield, D. A. Lipid peroxidation triggers neurodegeneration: a redox proteomics view into the Alzheimer disease brain. *Free Radic. Biol. Med.* ; 2012.
- [44] Banks, W. A.; Jaeger, L. B.; Urayama, A.; Kumar, V. B.; Hileman, S. M.; Gaskin, F. S.; Llanza, N. V.; Farr, S. A.; Morley, J. E. Preproenkephalin targeted antisense crosses the blood-brain barrier to reduce brain methionine enkephalin levels and increase voluntary ethanol drinking. *Peptides* **27**:784–796; 2006.
- [45] Jaeger, L. B.; Dohgu, S.; Hwang, M. C.; Farr, S. A.; Murphy, M. P.; Fleegal-DeMotta, M. A.; Lynch, J. L.; Robinson, S. M.; Niehoff, M. L.; Johnson, S. N.; Kumar, V. B.; Banks, W. A. Testing the neurovascular hypothesis of Alzheimer's disease: LRP-1 antisense reduces blood-brain barrier clearance, increases brain levels of amyloid- β protein, and impairs cognition. *J. Alzheimers Dis.* **17**:553–570; 2009.
- [46] Yamaguchi, H.; Ishiguro, K.; Uchida, T.; Takashima, A.; Lemere, C. A.; Imahori, K. Preferential labeling of Alzheimer neurofibrillary tangles with antisera for tau protein kinase (TPK I)/glycogen synthase kinase-3 β and cyclin-dependent kinase 5, a component of TPK II. *Acta Neuropathol.* **92**:232–241; 1996.
- [47] Pei, J. J.; Tanaka, T.; Tung, Y. C.; Braak, E.; Iqbal, K.; Grundke-Iqbal, I. Distribution, levels, and activity of glycogen synthase kinase-3 in the Alzheimer disease brain. *J. Neuropathol. Exp. Neurol.* **56**:70–78; 1997.
- [48] Leroy, K.; Yilmaz, Z.; Brion, J. P. Increased level of active GSK-3 β in Alzheimer's disease and accumulation in argyrophilic grains and in neurones at different stages of neurofibrillary degeneration. *Neuropathol. Appl. Neurobiol.* **33**:43–55; 2007.
- [49] Jope, R. S.; Yukaitis, C. J.; Beurel, E. Glycogen synthase kinase-3 (GSK3): Inflammation, diseases, and therapeutics. *Neurochem. Res.* **32**:577–595; 2007.
- [50] Wild, A. C.; Moinova, H. R.; Mulcahy, R. T. Regulation of gamma-glutamylcysteine synthetase subunit gene expression by the transcription factor Nrf2. *J. Biol. Chem.* **274**:33627–33636; 1999.
- [51] Itoh, K.; Chiba, T.; Takahashi, S.; Ishii, T.; Igarashi, K.; Katoh, Y.; Oyake, T.; Hayashi, N.; Satoh, K.; Hatayama, I.; Yamamoto, M.; Nabeshima, Y. An Nrf2/small Maf heterodimer mediates the induction of phase II detoxifying enzyme genes through antioxidant response elements. *Biochem. Biophys. Res. Commun.* **236**:313–322; 1997.
- [52] Malik, R.; Roy, I. Making sense of therapeutics using antisense technology. *Expert Opin. Drug Discov.* **6**:507–526; 2011.
- [53] Tamm, I. AEG-35156, an antisense oligonucleotide against X-linked inhibitor of apoptosis for potential treatment of cancer. *Curr. Opin. Investig. Drugs* **9**:638–646; 2008.
- [54] Petrusdottir, A. L.; Farr, S. A.; Morley, J. E.; Banks, W. A.; Skuladottir, G. V. Lipid peroxidation in brain during aging in the senescence-accelerated mouse (SAM). *Neurobiol. Aging* **28**:1170–1178; 2006.
- [55] Poon, H. F.; Joshi, G.; Sultana, R.; Farr, S. A.; Banks, W. A.; Morley, J. E.; Calabrese, V.; Butterfield, D. A. Antisense directed at the A β region of the APP decreases brain oxidative markers in aged senescence accelerated mice. *Brain Res.* **1018**:86–96; 2004.
- [56] Banks, W. A.; Farr, S. A.; Butt, W.; Kumar, V. B.; Franko, M. W.; Morley, J. E. Delivery across the blood-brain barrier of antisense directed against amyloid β : reversal of learning and memory deficits in mice overexpressing amyloid precursor protein. *J. Pharmacol. Exp. Ther.* **297**:1113–1121; 2001.
- [57] Kumar, V. B.; Farr, S. A.; Flood, J. F.; Kamlesh, V.; Franko, M.; Banks, W. A.; Morley, J. E. Site-directed antisense oligonucleotide decreases the expression of amyloid precursor protein and reverses deficits in learning and memory in aged SAMP8 mice. *Peptides* **21**:1769–1775; 2000.